

# Anle138b Modulates $\alpha$ -Synuclein Oligomerization and Prevents Motor Decline and Neurodegeneration in a Mouse Model of Multiple System Atrophy

Antonio Heras-Garvin, PhD <sup>1</sup>, Daniel Weckbecker, PhD,<sup>3</sup> Sergey Ryazanov, PhD,<sup>2</sup> Andrei Leonov, PhD,<sup>2,3</sup> Christian Griesinger, PhD,<sup>2</sup> Armin Giese, MD, PhD,<sup>4</sup> Gregor K. Wenning, MD, PhD<sup>1</sup> and Nadia Stefanova, MD, PhD <sup>1\*</sup>

<sup>1</sup>Department of Neurology, Division of Neurobiology, Medical University of Innsbruck, Innsbruck, Austria

<sup>2</sup>NMR Based Structural Biology, Max Planck Institute for Biophysical Chemistry, Göttingen, Germany

<sup>3</sup>MODAG GmbH, Wendelsheim, Germany

<sup>4</sup>Center for Neuropathology and Prion Research, Ludwig-Maximilians-Universität, Munich, Germany

**ABSTRACT: Background:** MSA is a fatal neurodegenerative disease characterized by autonomic failure and severe motor impairment. Its main pathological hallmark is the accumulation of  $\alpha$ -synuclein in oligodendrocytes, leading to glial and neuronal dysfunction and neurodegeneration. These features are recapitulated in the PLP- $\alpha$ Syn mouse model expressing human  $\alpha$ -synuclein in oligodendrocytes. At present, there is no effective disease-modifying therapy. Previous experiments have shown that the aggregation inhibitor, anle138b, reduces neurodegeneration and behavioral deficits in mouse models of other proteinopathies.

**Objectives:** To test the therapeutic potential of anle138b in a mouse model of MSA.

**Methods:** Two-month-old PLP- $\alpha$ Syn mice were fed over a period of 4 months with pellets containing anle138b at two different doses (0.6 and 2 g/kg) and compared to healthy controls and PLP- $\alpha$ Syn mice fed with placebo pellets. At the end of the treatment, behavioral and histological analyses were performed.

**Results:** We observed a reversal of motor function to healthy control levels when PLP- $\alpha$ Syn mice were treated with both doses of anle138b. Histological and molecular analyses showed a significant reduction in  $\alpha$ -synuclein oligomers and glial cytoplasmic inclusions in animals fed with anle138b compared to nontreated mice. These animals also present preservation of dopaminergic neurons and reduction in microglial activation in SN correlating with the  $\alpha$ -synuclein reduction observed.

**Conclusions:** Anle138b reduces  $\alpha$ -synuclein accumulation in PLP- $\alpha$ Syn mice, leading to neuroprotection, reduction of microglial activation, and preservation of motor function supporting the use of anle138b in a future clinical trial for MSA. © 2018 The Authors. *Movement Disorders* published by Wiley Periodicals, Inc. on behalf of International Parkinson and Movement Disorder Society.

**Key Words:**  $\alpha$ -synuclein; anle138b; movement disorders; multiple system atrophy; neurodegeneration

Multiple system atrophy (MSA) is a rare and progressive neurodegenerative disorder characterized by autonomic failure and severe motor impairment leading to death a few years after symptom onset.<sup>1</sup> No treatment

to stop or reduce disease progression is available; only mitigation of some clinical symptoms may be achieved.<sup>2</sup> MSA, together with Parkinson's disease (PD) and dementia with Lewy bodies, constitutes the family of

This is an open access article under the terms of the Creative Commons Attribution License, which permits use, distribution and reproduction in any medium, provided the original work is properly cited.

\***Correspondence to:** Dr. Nadia Stefanova, Division of Neurobiology, Department of Neurology, Medical University of Innsbruck, Innrain 66, 2nd floor, 6020 Innsbruck, Austria; E-mail: nadia.stefanova@i-med.ac.at

**Funding agencies:** The study was supported by grants of the Austrian Science Fund (FWF) I2102, under the frame of E-Rare-2, the ERA-Net for Research on Rare Diseases, Austrian Science Fund (FWF) F4414, and a grant of the European Community's Seventh Framework Programme (FP7/2007-2013) under agreement no. 602646 (Multisyn).

**Relevant conflicts of interests/financial disclosures:** S.R., A.L., A.G., and C.G. are inventors in a patent application related to the compound use in this study. A.G. and C.G. are shareholders and co-founders of MODAG GmbH. D.W. is fully and A.L. partly employed by MODAG.

Full financial disclosures and author roles may be found in the online version of this article.

**Received:** 24 May 2018; **Revised:** 23 October 2018; **Accepted:** 24 October 2018

**Published online 00 Month 2018 in Wiley Online Library (wileyonlinelibrary.com). DOI: 10.1002/mds.27562**

synucleinopathies, characterized by misfolding and accumulation of  $\alpha$ -synuclein ( $\alpha$ -syn).<sup>3-5</sup> In MSA,  $\alpha$ -syn accumulates in the cytoplasm of oligodendrocytes, forming the so-called glial cytoplasmic inclusions (GCIs), thus differing from PD where  $\alpha$ -syn mainly accumulates in neurons in Lewy bodies.<sup>3-5</sup>  $\alpha$ -syn accumulation in MSA leads to glial and neuronal dysfunction, neuroinflammation and finally neurodegeneration.<sup>1</sup> MSA is divided in two different subtypes depending on the main areas affected by neurodegeneration. The Parkinson's variant or MSA-P is characterized by striatonigral degeneration (SND), whereas the cerebellar variant or MSA-C reflects olivopontocerebellar atrophy (OPCA).<sup>1</sup> The PLP-h $\alpha$ Syn transgenic mouse model recapitulates most of the clinical and pathophysiological features of MSA by overexpressing human  $\alpha$ -syn under the oligodendrocyte PLP (myelin proteolipid protein) promoter, which leads to GCI formation, microglial activation, and selective neurodegeneration.<sup>6-16</sup>

Microglial activation and neuroinflammation constitute important pathological features of MSA.<sup>17-19</sup> Similarly to the human pathology, PLP-h $\alpha$ Syn mice develop progressive microglial activation, initially triggered by  $\alpha$ -syn pathology in a region-specific manner.<sup>13,15</sup> In a recent publication from our group, significant microglial activation was observed in the SN of MSA transgenic mice compared to healthy control animals at 5 months of age, and this activation was linked to abnormal neuroinflammatory response.<sup>15</sup> PLP-h $\alpha$ Syn mice also develop progressive SND characterized by a 30% reduction in the number of dopaminergic neurons (tyrosine hydroxylase positive [TH<sup>+</sup>] neurons) in the SNc compared to healthy control animals. This neuronal loss is already present at 4 months of age and is followed by a significant reduction in density of dopaminergic terminals and in number of medium spiny neurons in the striatum at 12 months of age.<sup>15,20</sup> SN and striatum are both essential for motor control, and the loss of neurons in these two brain areas leads to motor impairment in these mice.<sup>12,15</sup>

According to several studies, under physiological conditions  $\alpha$ -syn is mainly located in the pre-synaptic terminals of the neurons predominantly as a monomer.<sup>21</sup> Although its function is still unknown, a possible role in neurotransmitter release, synaptic function, and plasticity has been suggested.<sup>22,23</sup> Misfolding, oligomerization, and aggregation of  $\alpha$ -syn are crucial events in the pathophysiology of synucleinopathies.<sup>24</sup> In MSA, the origin of  $\alpha$ -syn inclusions in oligodendrocytes is still unknown and under discussion given that it is not clear whether or not mature oligodendrocytes express  $\alpha$ -syn.<sup>25-27</sup> In the last years, several publications have shown the ability of  $\alpha$ -syn to be transferred from cell to cell and spread through brain parenchyma in a prion-like manner.<sup>28-33</sup> Based on this, possible neuron-oligodendrocyte transfer of  $\alpha$ -syn has been suggested in

addition to the controversial oligodendrocytic origin of the misfolded  $\alpha$ -syn.<sup>34</sup> Several studies in the last few years have shown that  $\alpha$ -syn oligomers constitute the main neurotoxic species for disease progression instead of large fibrillar deposits or inclusions.<sup>35-39</sup> According to all these studies, the inhibition of  $\alpha$ -syn oligomerization constitutes a promising approach to fight the spreading of synucleinopathies and an important effort has been made in this direction.<sup>21,40,41</sup> The use of small molecules to target  $\alpha$ -syn oligomerization and aggregation has shown promising results in preclinical models of PD as is the case of anle138b, a small compound with high bioavailability and low toxicity.<sup>42</sup> This compound can be delivered orally and penetrates the blood-brain barrier, entering the brain with high efficacy.<sup>42</sup> Thus, administration of anle138b as a food additive results in adequate and stable drug exposure.<sup>43</sup> Anle138b has been shown effective in reducing disease progression in models of PD, prion disease, tauopathy, and Alzheimer's disease (AD) by inhibiting protein aggregation.<sup>42-45</sup> Based on this, we hypothesized that it could also be of use to attenuate disease progression in MSA. In order to test this hypothesis, we fed PLP-h $\alpha$ Syn transgenic MSA mice with food pellets containing two different doses of anle138b followed by behavioral and histological analyses at the end of the treatment.

## Material and Methods

### Animals and Treatments

PLP-h $\alpha$ Syn mice overexpressing wild-type (WT) human  $\alpha$ -syn under the PLP promoter, an oligodendroglial-specific promoter, and generated in a C57/BL6 background<sup>16</sup> were used in this study. Animals were kept under temperature-controlled, pathogen-free conditions on a light/dark 12-hour cycle. All the experiments were performed according to the ethical guidelines with the permission of the Austrian Federal Ministry of Science and Research (permission BMFWF-66.011/0141-WF/v/3b/2016). Two-month-old male transgenic mice were randomized in three different groups: one fed with placebo food pellets (n = 10; ssniff Spezialdiäten GmbH, Soest, Germany), another fed with pellets containing anle138b at 0.6 g/kg of food (n = 8; ssniff Spezialdiäten GmbH), and a last group fed with pellets containing 2 g of anle138b per kg of food (n = 10; ssniff Spezialdiäten GmbH). The dose of 2 g of anle138b per kg of food was used in previous experiments in mice<sup>43</sup> and establishes during the wake phase a concentration of 60  $\mu$ M in the brain. Two-month-old C57/BL6 healthy nontransgenic animals (WT) fed with placebo pellets were used as a healthy control (n = 10). Food pellets were provided to the animals throughout the whole experiment. After 4 months of treatment, behavioral analyses were performed followed by sacrifice of the animals and brain extraction.

## Behavioral Tests

### Challenging Beam Test

At the end of the treatment, animal cages were randomly numbered by the animal caretaker and behavioral analyses were performed by the researcher blinded to genotype and treatment. Motor performance and coordination were analyzed with a modified version of the traditional beam test adapted from a previously published method.<sup>46,47</sup> Five performances were video recorded per animal, and the number of slips per step with the hind limbs was measured. The best three performances were used for statistical analyses.

### Tissue Processing and Histology

After behavioral analyses were performed, animals were perfused intracardially with phosphate buffered saline (PBS [pH 7.4]; Sigma-Aldrich, St. Louis, MO) under deep thiopental anesthesia and brains were extracted. For molecular analyses, brains were snap frozen in liquid nitrogen and stored at  $-80^{\circ}\text{C}$ . For histological analyses, brains were postfixed overnight in 4% paraformaldehyde (pH 7.4; Sigma-Aldrich) at  $4^{\circ}\text{C}$ . After fixation, brains were washed in PBS and then transferred to 30% sucrose (in PBS) until they sank. Finally, brains were frozen using 2-methylbutan (Sigma-Aldrich) and stored at  $-80^{\circ}\text{C}$  for further analyses. In order to perform histological analyses, brains were serially cut in  $40\text{-}\mu\text{m}$ -thick coronal sections using a freezing microtome (Leica Microsystems, Wetzlar, Germany) and stored free-floating in a cryoprotectant buffer at  $-20^{\circ}\text{C}$ . One series was directly mounted on slides and stained with cresyl violet.

### Immunohistological Analyses

Free-floating sections were stained following standard protocols. To analyze the number of GCIs, representative sections, including striatum and SN, were stained with the following antibodies: rat antihuman  $\alpha\text{-syn}$  15G7 (1:200; Enzo Life Sciences, Farmingdale, NY) and mouse antioligomeric human  $\alpha\text{-syn}$  5G4 (1:1,000; LINARIS GmbH, Mannheim, Germany). To analyze the number of dopaminergic neurons ( $\text{TH}^+$  neurons) in the SNc, serial sections were stained with rabbit anti-TH antibody (1:1,000; Millipore, Burlington, MA). For microglial activation analysis, representative sections of SN were stained with rat anti-CD68 antibody (1:200; R&D Systems, Minneapolis, MN). Sections were then incubated with biotinylated secondary antibodies, followed by Vectastain ABC reagent (Vector Laboratories, Burlingame, CA) and 3,3'-diaminobenzidine (Sigma-Aldrich), to visualize the immunohistochemical binding sites. Stained sections were mounted on slides, dehydrated, and coverslipped with Entellan (Merck & Co., Merck Kenilworth, NJ). For immunofluorescence,

suitable immunoglobulin Gs, conjugated with Alexa 488 or Alexa 594 (Life Technologies, Carlsbad, CA), were applied, followed by nuclear staining with 4',6-diamidino-2-phenylindole (1:1,000; Sigma-Aldrich) and finally coverslipped with mounting medium Fluoromount-G (SouthernBiotech, Birmingham, AL).

### Image Analyses

After immunostaining, and preceding the acquisition of images/stereological counting, all immunofluorescence/immunohistochemistry slides were randomly numbered by the laboratory technician. All measurements were therefore performed by the researcher blinded to genotype and treatment. Neuroanatomy was assessed using a Mouse Brain Atlas. Stereological analysis was performed using the Nikon E-800 microscope equipped with a Nikon digital camera DXM1200 (Nikon, Tokyo, Japan) and Stereoinvestigator software (Microbrightfield Europe E.k., Magdeburg, Germany) as described previously.<sup>48</sup> GCI density was assessed by meander scan throughout the area of interest and expressed in number of GCI/ $\text{mm}^2$ . The number of  $\text{TH}^+$  and cresyl violet positive ( $\text{CV}^+$ ) neurons in the SNc was measured by applying the optical fractionator workflow. For microglial activation assessment, images were acquired with a fluorescence microscope (Leica DMI4000; Leica Microsystems), and the CD68-positive area was estimated using ImageJ software (National Institutes of Health, Bethesda, MD). Results are presented as percentage of CD68 area per SN area.

### Continuous Sucrose-Gradient Assay

For continuous gradient centrifugation, a 10% (w/v) brain homogenate of the midbrain was prepared using a buffer composed of 50 mM of Tris (pH 7.4), 175 mM of NaCl, 1 mM of  $\text{MgCl}_2$ , 0.1 mM of phenylmethylsulfonyl fluoride, 1 mM of N-ethylmaleimide, 0.1% Nonidet P-40 Substitute, ethylenediaminetetraacetic acid-free cOmplete Mini protease inhibitor (Roche, Indianapolis, IN), and PhosSTOP phosphatase inhibitor (Roche). Aliquots of the homogenate were frozen in liquid  $\text{N}_2$  and stored at  $-80^{\circ}\text{C}$ . Total protein concentration was determined by bicinchoninic acid assay. For the sucrose gradient analysis, 300  $\mu\text{g}$  of protein in a final volume of 200  $\mu\text{L}$  were used. To this end, the brain homogenate was thawed on ice and diluted in a buffer containing 50 mM of Tris (pH 7.4), 175 mM of NaCl, 0.1% N-lauroylsarcosine sodium salt (sarcosyl), and 0.5% sodium deoxycholate. Samples were agitated at 1,200 rpm (ThermoMixer C, Eppendorf) at  $4^{\circ}\text{C}$  for 30 minutes. Cellular debris was removed afterward by centrifugation for 1 minute at 16,000 g and  $4^{\circ}\text{C}$ . Sucrose gradients were prepared in a 4-mL  $11 \times 60$  mm polyallomer tube (Beckman Coulter, Brea, CA). To this end, sucrose solutions containing 50 mM

of Tris (pH 7.4), 0.1% sarcosyl, and 10%, 20%, 30%, 40%, 50%, or 60% of sucrose were pipetted into the tube, starting with 200  $\mu$ L of the 60% sucrose solution and followed by 400  $\mu$ L of the 50% to 10% sucrose solutions. Two hundred microliters of the centrifugation supernatant was pipetted as the uppermost layer onto the gradient. Samples were ultracentrifuged in a SW 60 Ti rotor (Beckman Coulter) at 40,000 rpm and 4  $^{\circ}$ C for 1 hour. Twelve fractions of 200  $\mu$ L each were collected from the top to the bottom of each tube and subjected to trichloroacetic acid (TCA) precipitation (10% TCA) overnight at  $-20^{\circ}$ C. After thawing, samples were centrifuged at 25,000 g and 4  $^{\circ}$ C for 15 minutes. Precipitates were washed once with acetone ( $-20^{\circ}$ C), centrifuged, and finally resuspended in Laemmli sample buffer. Samples were boiled at 96  $^{\circ}$ C for 5 minutes and subjected to sodium dodecyl sulfate polyacrylamide gel electrophoresis and western blotting. Antibodies against total  $\alpha$ -syn (4B12; BioLegend, San Diego, CA) and phosphorylated  $\alpha$ -syn (pS129; Abcam, Cambridge, MA) were used to stain the blots. Images were acquired using the Fusion FX system for western blot and gel imaging, and quantified with FUSION CAPT software (V16.09b; Vilber Lourmat Sté, Collégien, France).

### Statistical Analyses

All statistical analyses were conducted using the software Graph-Pad Prism (version 7; GraphPad Software Inc., La Jolla, CA). Mean  $\pm$  standard error of the mean (SEM) was used to present the results. One-way analysis of variance (ANOVA) with a post-hoc Bonferroni test was used to compare groups if not indicated otherwise. A  $P$  value  $<0.05$  was considered statistically significant. Correlations were studied using linear regression analysis.

## Results

### Anle138b Prevents Motor Deficits and Neurodegeneration in the PLP- $\alpha$ Syn Mice

To assess the effect of anle138b on motor function, motor coordination and balance were analyzed using the beam challenging test<sup>46,47</sup> (Fig. 1). PLP- $\alpha$ Syn mice fed with placebo pellets showed a significant increase in the number of slips per step when traversing the beam compared to healthy control animals (Fig. 1). However, PLP- $\alpha$ Syn mice treated with both doses of anle138b maintained normal motor function as compared to healthy control mice (Fig. 1).

To evaluate whether the improvement in motor function was related to a neuroprotective effect of anle138b on dopaminergic neurons in the SNc, the number of TH<sup>+</sup> cells was quantified in this region. Stereological counting showed a clear preservation of dopaminergic

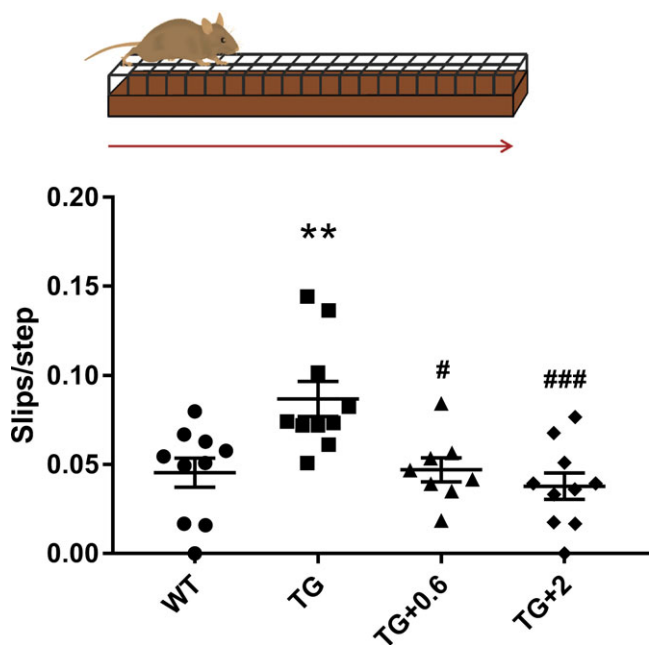


**FIG. 1.** Anle138b treatment prevents motor impairment in PLP- $\alpha$ Syn mice. Schematic representation of the beam challenge test used for behavioral analysis. The number of slips when the animals traverse the beam were counted and normalized per the number of steps.  $n = 8$  to 10 per experimental group. Error bars indicate SEM. ANOVA, slips per step/genotype: \*\* $P < 0.01$ ; Slips per step/treatment: # $P < 0.05$ ; ### $P < 0.001$  (Bonferroni's test). WT, wild-type healthy control animals; TG, PLP- $\alpha$ Syn mice fed with placebo food pellets; TG + 0.6, PLP- $\alpha$ Syn mice fed with pellets containing anle138b at 0.6 g/kg of food; TG + 2, PLP- $\alpha$ Syn mice fed with pellets containing anle138b at 2 g/kg of food. [Color figure can be viewed at [wileyonlinelibrary.com](http://wileyonlinelibrary.com)]

neurons in the SNc of PLP- $\alpha$ Syn mice treated with both doses of anle138b compared to healthy controls (Fig. 2A,B). PLP- $\alpha$ Syn mice fed with placebo pellets, however, showed a significant loss of TH<sup>+</sup> neurons compared to all groups (Fig. 2A,B). The neuroprotective effect of anle138b in SNc was validated by cresyl violet staining followed by stereological counting of neurons in this brain area (Supporting Information Fig. S1A). There was a significant correlation between the neuroprotective effect of anle138b and improvement in motor function (Fig. 2C and Supporting Information Fig. S1B).

### Anle138b Reduces $\alpha$ -Syn Accumulation in PLP- $\alpha$ Syn Mice

Next, the effect of anle138b on  $\alpha$ -syn aggregation and intracellular accumulation was assessed. Brain sections of PLP- $\alpha$ Syn mice were immunostained by using antibodies against  $\alpha$ -syn, and the number of GCIs per area in striatum and SN was analyzed. Both doses of anle138b showed a significant effect on GCI number in SNc and striatum, where a 30% reduction was observed (Fig. 3A–C and Supporting Information Fig. S2A,B). This effect was confirmed with the different antibodies used in the study (Fig. 3A–C and Supporting Information

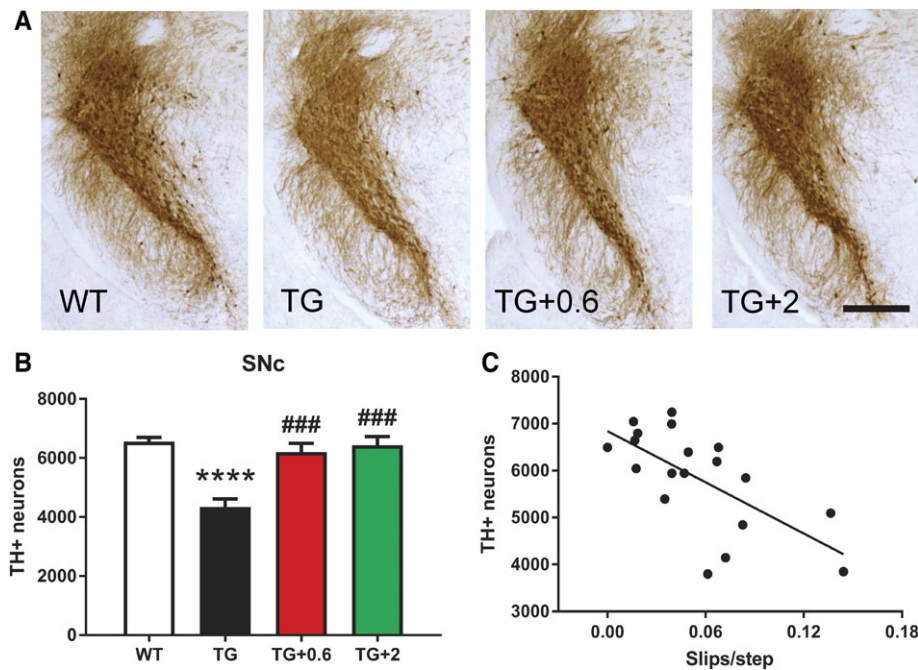


**FIG. 2.** Anle138b prevents dopaminergic neuronal loss in the SNc of PLP-h $\alpha$ Syn mice. (A) Representative images of SN sections stained against TH. Scale bar, 400  $\mu$ m. (B) Stereological counting of the total number of dopaminergic (TH<sup>+</sup>) neurons in the entire SNc in the different groups.  $n = 4$  to 5 per experimental group. Error bars indicate SEM. ANOVA, TH<sup>+</sup> neurons/genotype: \*\*\*\* $P < 0.0001$ ; TH<sup>+</sup> neurons/treatment: ### $P < 0.001$  (Bonferroni's test). (C), Correlation analysis of number of TH<sup>+</sup> neurons in the SNc and number of slips per step.  $P = 0.0021$ ;  $R^2 = 0.4349$ . [Color figure can be viewed at [wileyonlinelibrary.com](http://wileyonlinelibrary.com)]

Fig. S2A,B). There was a significant correlation between GCI reduction and preservation of neurons in SNc (Fig. 3D and Supporting Information Fig. S1C,D and S2C) as well as motor function (Fig. 3E and Supporting Information Fig. S2D).

In addition to the effect on the amount of GCIs, sucrose-gradient analysis showed a significant reduction of  $\alpha$ -syn oligomers in midbrains of PLP-h $\alpha$ Syn mice treated with anle138b (Fig. 3F,G). This reduction was observed not only in total  $\alpha$ -syn oligomers, but also in pathological phosphorylated  $\alpha$ -syn oligomers (Fig. 3F, G), thus confirming the modulatory effect of the small molecule on  $\alpha$ -syn oligomerization.

### Anle138b Reduces Microglial Activation in PLP-h $\alpha$ Syn Mice

To assess the effect of anle138b treatment on microglial activation, we performed immunofluorescence microscopy for CD68, a lysosomal marker indicative of phagocytic activity of microglia<sup>49</sup> associated with  $\alpha$ -syn accumulation.<sup>15,50-52</sup> In agreement with previous results,<sup>15</sup> significant microglial activation was observed at this stage in the SN of the PLP-h $\alpha$ Syn placebo group compared to healthy control animals (Fig. 4A,B). In contrast, both doses of anle138b significantly reduced microglial activation in the SN back to its normal levels as observed in healthy control mice (Fig. 4A,B). There was a significant correlation between the reduction of microglial activation in SN, GCI reduction (Fig. 4C and

Supporting Information Fig. S2E), preservation of neurons (Fig. 4D and Supporting Information Fig. S1E), as well as motor function (Fig. 4E).

## Discussion

Aggregation and accumulation of misfolded proteins constitute a key factor in the progression of several neurodegenerative diseases. Thus, the use of compounds or therapies capable of reducing or blocking abnormal protein aggregation represents a promising strategy to attenuate the clinical progression in these disorders. Synucleinopathies are pathologically characterized by the abnormal aggregation and accumulation of  $\alpha$ -syn, and, in recent years, different approaches have been developed to target this process.<sup>3-5,21,40,41</sup> The use of small molecules and immunotherapy constitute two of the main strategies with therapeutic potential according to preclinical in vivo and in vitro models.<sup>53,54</sup> Small molecules present important advantages such as their high oral bioavailability and blood-brain barrier penetration and their ability to act inside cells.<sup>53</sup>

Here we show that anle138b, which targets specifically oligomers, reduces  $\alpha$ -syn accumulation in a mouse model of early-stage MSA, thus corroborating the oligomer modulation effect on  $\alpha$ -syn previously observed in PD models and the general effect observed also in Abeta, tau, and prion aggregation mouse models.<sup>42-45</sup> An important advantage of this small molecule, from a

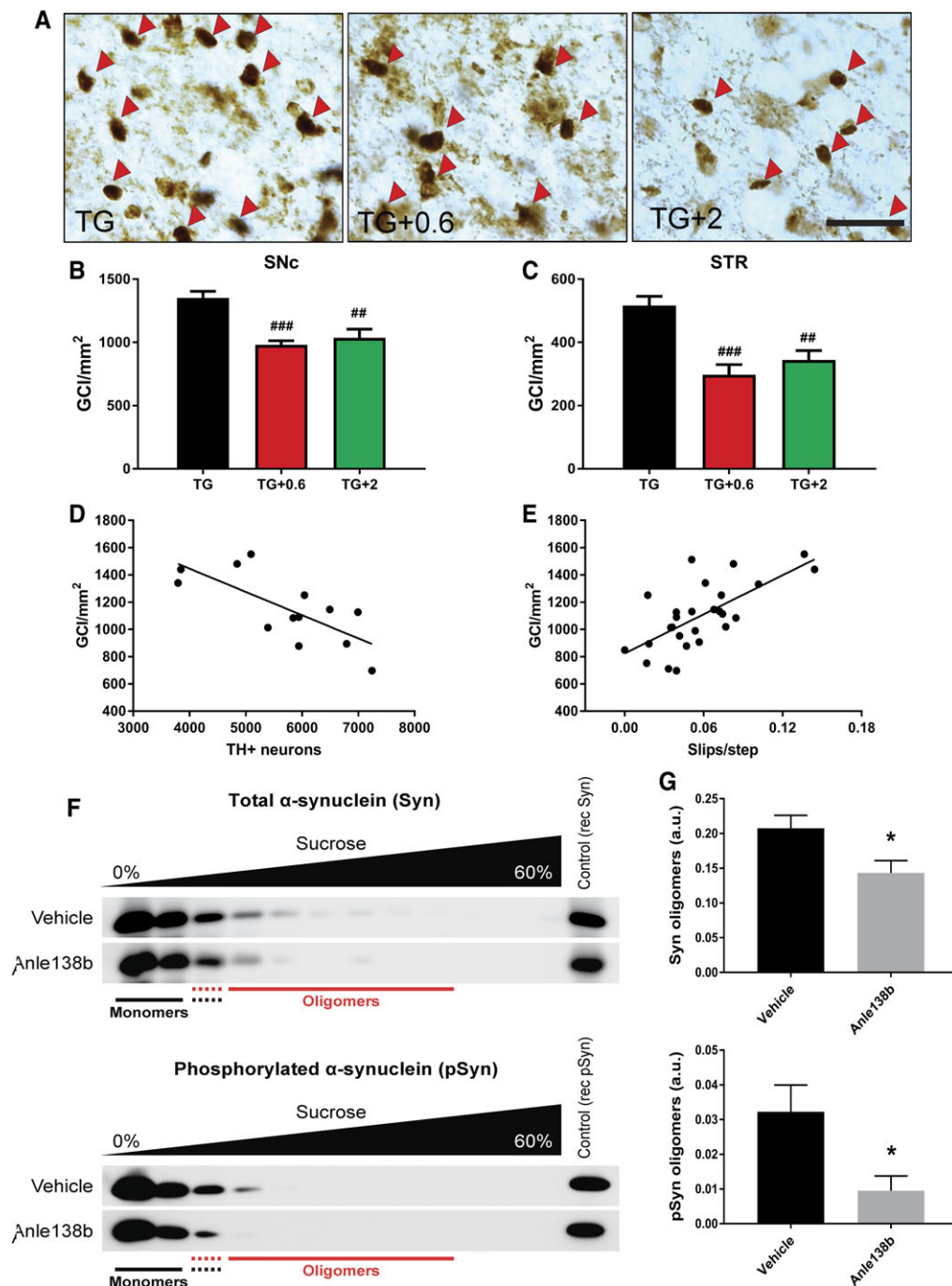


**FIG. 3.** Anle138b reduces  $\alpha$ -syn accumulation in PLP-haSyn mice (A) Representative images of striatal sections stained with the antibody 15G7 against human  $\alpha$ -syn. Red arrows indicate individual GCI. Scale bar, 25  $\mu$ m. (B,C) GCI density in SNc and STR (striatum) of PLP-haSyn mice determined by stereological counting of brain sections stained with 15G7 and expressed in GCI/mm<sup>2</sup>.  $n = 8$  to 10 per experimental group. Error bars indicate SEM. ANOVA, GCI density/treatment: ## $P < 0.01$ ; ### $P < 0.001$  (Bonferroni's test). (D) Correlation analysis between the density of GCIs in the SNc and the number of TH<sup>+</sup> neurons in the same region.  $P = 0.0041$ ;  $R^2 = 0.5415$ . (E) Correlation analysis of density of GCIs in the SNc and number of slips per step.  $P = 0.0001$ ;  $R^2 = 0.4546$ . (F) Representative blots of midbrain samples obtained after sucrose-gradient centrifugation. Total  $\alpha$ -syn (upper panel) and phosphorylated  $\alpha$ -syn (lower panel) levels were analyzed in the different fractions. (G) Quantification of total  $\alpha$ -syn (upper panel) and phosphorylated  $\alpha$ -syn (lower panel) levels in the oligomeric fractions.  $n = 4$  per experimental group. Error bars indicate SEM. Groups were compared by unpaired two-tailed  $t$  test. \* $P < 0.05$ . [Color figure can be viewed at [wileyonlinelibrary.com](http://wileyonlinelibrary.com)]

therapeutic point of view, is that it does not bind to  $\alpha$ -syn monomers, therefore preserving its physiological functions.<sup>42</sup> At the molecular level, anle138b blocks the formation of toxic  $\alpha$ -syn oligomers,<sup>42</sup> which, in

pathological conditions, can induce neuronal damage through the formation of pores in the cell membrane and mitochondria<sup>21,39,55,56</sup> and trigger the activation of microglial cells.<sup>52,57-59</sup> Because formation of  $\alpha$ -syn

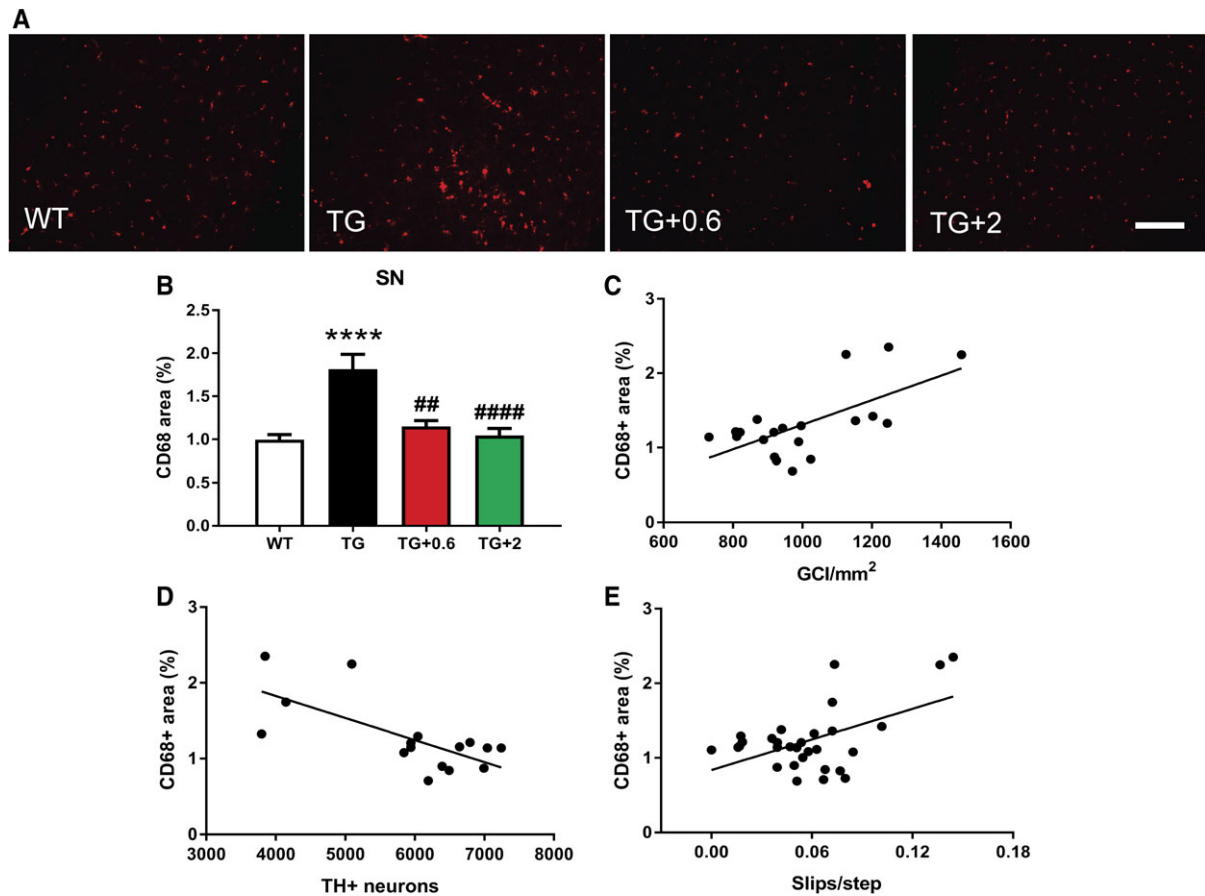


**FIG. 4.** Anle138b reduces microglial activation in PLP-h $\alpha$ Syn mice. (A) Representative immunofluorescence images of SN sections stained against CD68. Scale bar, 150  $\mu$ m. (B) CD68-positive (CD68<sup>+</sup>) area in the different groups, determined by ImageJ analysis (National Institutes of Health, Bethesda, MD) and expressed as the % of the total area of the SN.  $n = 6$  to 9 per experimental group. Error bars indicate SEM. ANOVA, CD68<sup>+</sup> area/genotype: \*\*\*\* $P < 0.0001$ ; CD68<sup>+</sup> area/treatment: ## $P < 0.01$ ; #### $P < 0.0001$  (Bonferroni's test). (C) Correlation analysis of CD68<sup>+</sup> area in the SN and density of GCIs (15G7) in the same brain region.  $P = 0.0017$ ;  $R^2 = 0.4288$ . (D) Correlation analysis between the CD68<sup>+</sup> area in the SN and the number of TH<sup>+</sup> neurons in the SNc.  $P = 0.0027$ ;  $R^2 = 0.4862$ . (E) Correlation analysis of CD68<sup>+</sup> area in the SN and number of slips per step.  $P = 0.0033$ ;  $R^2 = 0.2689$ . [Color figure can be viewed at [wileyonlinelibrary.com](http://wileyonlinelibrary.com)]

oligomers is blocked, also less  $\alpha$ -syn fibrils are generated. In accord with this, our data show that oral administration of anle138b reduces  $\alpha$ -syn oligomers in midbrains of PLP-h $\alpha$ Syn mice and leads to a 30% reduction in the number of GCI in the striatum and SN of MSA mice, two brain areas associated with motor function. We also demonstrate that the reduction of  $\alpha$ -syn accumulation prevents loss of dopaminergic nigral neurons and motor impairment, thus confirming the therapeutic effect of anle138b observed also in PD models.<sup>42,44</sup> Finally, our data show that the decrease of  $\alpha$ -syn aggregation in the SN is associated with a reduction of microglial activation back to the levels observed in healthy control animals in this brain region, which also correlates with the neuroprotective effect of anle138b on dopaminergic cells and preservation of motor function.

The results presented here demonstrate that anle138b treatment is beneficial in early-stage MSA as modeled by young PLP-h $\alpha$ Syn mice.<sup>15</sup> However, efficacy of anle138b was less prominent in a model of pathologically

advanced MSA.<sup>60</sup> In that study, the potential of anle138b was evaluated in 1-year-old PLP-h $\alpha$ Syn mice treated with the mitochondrial toxin, 3-nitropropionic acid (3-NP), to trigger full-blown MSA-like pathology, with spreading of GCI, SND, and OPCA and strong microglial activation.<sup>12</sup> Behavioral analyses showed significant motor improvement after short-term treatment with anle138b; however, no significant changes in  $\alpha$ -syn aggregate load or cell death were observed in these animals.<sup>60</sup> The variable efficacy of anle138b in the two studies may be attributed to short (1 month) versus long-term (4 months) treatment, but also reflect the fact that PLP-h $\alpha$ Syn animals had sustained different degrees of neurodegeneration in the absence or presence of 3-NP exposure. Moreover, the limited efficacy of anle138b in our first experiment may have been attributed to the addition of toxin-induced acute oxidative stress that cannot be counteracted by the administration of anle138b, given that it has no antioxidant properties. In contrast, to clarify the antiaggregation and neuroprotective potential of anle138b, a different, preventive approach was used in

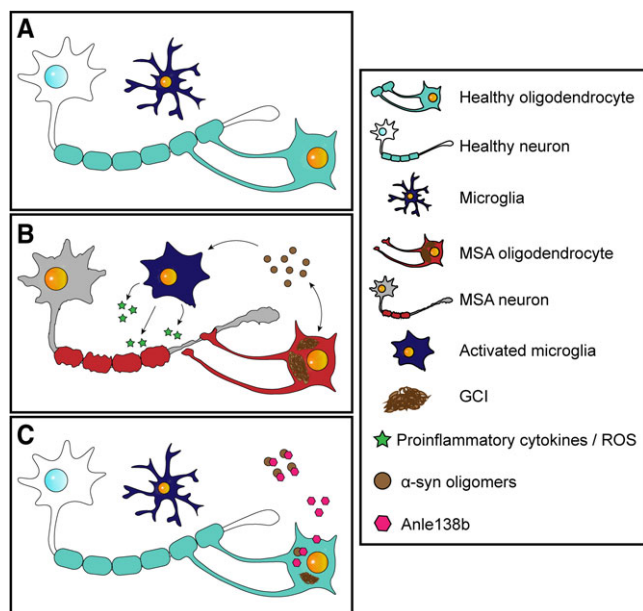


**FIG. 5.** Pathophysiological features of MSA and potential therapeutic effect of anle138b. (A) Schematic overview of the CNS in healthy conditions. (B) During MSA pathogenesis  $\alpha$ -syn accumulates in the cytoplasm of oligodendrocytes inducing oligodendroglial dysfunction. Toxic oligomeric species of  $\alpha$ -syn are also formed and spread through the brain parenchyma triggering microglial activation and neuroinflammation. All these events lead finally to demyelination and neurodegeneration. (C) Treatment with anle138b would reduce the formation of GCIs and other toxic  $\alpha$ -syn species and would attenuate neuroinflammation, demyelination, and neurodegeneration in MSA patients. [Color figure can be viewed at [wileyonlinelibrary.com](http://wileyonlinelibrary.com)]

the present study, where chronic administration of the compound started before nigral degeneration of dopaminergic neurons occurred and in the absence of other non- $\alpha$ Syn-dependent deleterious stimuli.

In summary, our study shows that oral administration of anle138b with initiation in the early disease stages constitutes a promising approach to prevent disease progression in MSA (Fig. 5). Our observations and previous studies have demonstrated the potential of anle138b in different neurodegenerative disorders, and the data presented here support further development of anle138b for future clinical applications in patients suffering from MSA or related synucleinopathies. ■

**Acknowledgments:** The study was supported by grants of the Austrian Science Fund (FWF) I2102, F4414, and a grant of the European Community's Seventh Framework Programme (FP7/2007-2013) under agreement n 602646 (Multisyn).

## References

- Fanciulli A, Wenning GK. Multiple-system atrophy. *N Engl J Med* 2015;372:249–263.
- Eschlbock S, Krismer F, Wenning GK. Interventional trials in atypical parkinsonism. *Parkinsonism Relat Disord* 2016;22(Suppl 1):S82–S92.
- Spillantini MG, Schmidt ML, Lee VM, Trojanowski JQ, Jakes R, Goedert M. Alpha-synuclein in Lewy bodies. *Nature* 1997;388:839–40.
- Trojanowski JQ, Lee VM. Parkinson's disease and related alpha-synucleinopathies are brain amyloidoses. *Ann N Y Acad Sci* 2003;991:107–110.
- Tu PH, Galvin JE, Baba M, et al. Glial cytoplasmic inclusions in white matter oligodendrocytes of multiple system atrophy brains contain insoluble alpha-synuclein. *Ann Neurol* 1998;44:415–422.
- Boudes M, Uvin P, Pinto S, et al. Bladder dysfunction in a transgenic mouse model of multiple system atrophy. *Mov Disord* 2013;28:347–355.
- Fernagut PO, Meissner WG, Biran M, et al. Age-related motor dysfunction and neuropathology in a transgenic mouse model of multiple system atrophy. *Synapse*. 2014;68:98–106.
- Flabeau O, Meissner WG, Ozier A, Berger P, Tison F, Fernagut PO. Breathing variability and brainstem serotonergic loss in a genetic model of multiple system atrophy. *Mov Disord* 2014;29:388–395.
- Hartner L, Keil TW, Kreuzer M, et al. Distinct parameters in the EEG of the PLP alpha-SYN mouse model for multiple system atrophy reinforce face validity. *Front Behav Neurosci* 2016;10:252.
- Krismer F, Wenning GK, Li Y, Poewe W, Stefanova N. Intact olfaction in a mouse model of multiple system atrophy. *PLoS One* 2013;8:e64625.
- Kuzdas D, Stemberger S, Gaburro S, Stefanova N, Singewald N, Wenning GK. Oligodendroglial alpha-synucleinopathy and MSA-like cardiovascular autonomic failure: experimental evidence. *Exp Neurol* 2013;247:531–536.
- Stefanova N, Reindl M, Neumann M, et al. Oxidative stress in transgenic mice with oligodendroglial alpha-synuclein overexpression replicates the characteristic neuropathology of multiple system atrophy. *Am J Pathol* 2005;166:869–876.
- Stefanova N, Reindl M, Neumann M, Kahle PJ, Poewe W, Wenning GK. Microglial activation mediates neurodegeneration related to oligodendroglial alpha-synucleinopathy: implications for multiple system atrophy. *Mov Disord* 2007;22:2196–2203.
- Stemberger S, Poewe W, Wenning GK, Stefanova N. Targeted overexpression of human alpha-synuclein in oligodendroglia induces lesions linked to MSA-like progressive autonomic failure. *Exp Neurol* 2010;224:459–464.
- Refolo V, Bez F, Polissidis A, et al. Progressive striatonigral degeneration in a transgenic mouse model of multiple system atrophy: translational implications for interventional therapies. *Acta Neuropathol Commun* 2018;6:2. doi: <https://doi.org/10.1186/s40478-017-0504-y>.
- Kahle PJ, Neumann M, Ozmen L, et al. Hyperphosphorylation and insolubility of alpha-synuclein in transgenic mouse oligodendrocytes. *EMBO Rep* 2002;3:583–588.
- Gerhard A, Banati RB, Goerres GB, et al. [11C](R)-PK11195 PET imaging of microglial activation in multiple system atrophy. *Neurology* 2003;61:686–689.
- Vieira BD, Radford RA, Chung RS, Guillemin GJ, Pountney DL. Neuroinflammation in multiple system atrophy: response to and cause of alpha-synuclein aggregation. *Front Cell Neurosci* 2015;9:437.
- Ishizawa K, Komori T, Sasaki S, Arai N, Mizutani T, Hirose T. Microglial activation parallels system degeneration in multiple system atrophy. *J Neuropathol Exp Neurol* 2004;63:43–52.
- Bassil F, Fernagut PO, Bezaud E, et al. Reducing C-terminal truncation mitigates synucleinopathy and neurodegeneration in a transgenic model of multiple system atrophy. *Proc Natl Acad Sci U S A* 2016;113:9593–9598.
- Lashuel HA, Overk CR, Oueslati A, Maslah E. The many faces of alpha-synuclein: from structure and toxicity to therapeutic target. *Nat Rev Neurosci* 2013;14:38–48.
- Bendor JT, Logan TP, Edwards RH. The function of alpha-synuclein. *Neuron* 2013;79:1044–1066.
- Burre J, Sharma M, Tsetsenis T, Buchman V, Etherton MR, Sudhof TC. Alpha-synuclein promotes SNARE-complex assembly in vivo and in vitro. *Science* 2010;329:1663–1667.
- Wong YC, Kraic D. alpha-synuclein toxicity in neurodegeneration: mechanism and therapeutic strategies. *Nat Med* 2017;23:1–13.
- Asi YT, Simpson JE, Heath PR, et al. Alpha-synuclein mRNA expression in oligodendrocytes in MSA. *Glia* 2014;62:964–970.

26. Djelloul M, Holmqvist S, Boza-Serrano A, et al. Alpha-synuclein expression in the oligodendrocyte lineage: an in vitro and in vivo study using rodent and human models. *Stem Cell Reports* 2015;5:174–184.
27. Miller DW, Johnson JM, Solano SM, Hollingsworth ZR, Standaert DG, Young AB. Absence of alpha-synuclein mRNA expression in normal and multiple system atrophy oligodendroglia. *J Neural Transm (Vienna)* 2005;112:1613–1624.
28. Kordower JH, Chu Y, Hauser RA, Freeman TB, Olanow CW. Lewy body-like pathology in long-term embryonic nigral transplants in Parkinson's disease. *Nat Med* 2008;14:504–506.
29. Kovacs GG, Breydo L, Green R, Kis V, Puska G, Lorincz P, et al. Intracellular processing of disease-associated alpha-synuclein in the human brain suggests prion-like cell-to-cell spread. *Neurobiol Dis* 2014;69:76–92.
30. Recasens A, Dehay B, Bove J, et al. Lewy body extracts from Parkinson disease brains trigger alpha-synuclein pathology and neurodegeneration in mice and monkeys. *Ann Neurol* 2014;75:351–362.
31. Luk KC, Kehm V, Carroll J, et al. Pathological alpha-synuclein transmission initiates Parkinson-like neurodegeneration in nontransgenic mice. *Science* 2012;338:949–953.
32. Watts JC, Giles K, Oehler A, et al. Transmission of multiple system atrophy prions to transgenic mice. *Proc Natl Acad Sci U S A* 2013;110:19555–19560.
33. Peelaerts W, Bousset L, Van der Perren A, et al. alpha-Synuclein strains cause distinct synucleinopathies after local and systemic administration. *Nature* 2015;522:340–344.
34. Reyes JF, Rey NL, Bousset L, Melki R, Brundin P, Angot E. Alpha-synuclein transfers from neurons to oligodendrocytes. *Glia* 2014;62:387–398.
35. Kalia LV, Kalia SK, McLean PJ, Lozano AM, Lang AE. alpha-Synuclein oligomers and clinical implications for Parkinson disease. *Ann Neurol* 2013;73:155–169.
36. Winner B, Jappelli R, Maji SK, et al. In vivo demonstration that alpha-synuclein oligomers are toxic. *Proc Natl Acad Sci U S A* 2011;108:4194–4199.
37. Volles MJ, Lansbury PT, Jr. Zeroing in on the pathogenic form of alpha-synuclein and its mechanism of neurotoxicity in Parkinson's disease. *Biochemistry* 2003;42:7871–7878.
38. Outeiro TF, Putcha P, Tetzlaff JE, Spoelgen R, Koker M, Carvalho F, et al. Formation of toxic oligomeric alpha-synuclein species in living cells. *PLoS One* 2008;3:e1867.
39. Kostka M, Hogen T, Danzer KM, et al. Single particle characterization of iron-induced pore-forming alpha-synuclein oligomers. *J Biol Chem* 2008;283:10992–11003.
40. Eisele YS, Monteiro C, Fearn C, et al. Targeting protein aggregation for the treatment of degenerative diseases. *Nat Rev Drug Discov* 2015;14:759–780.
41. Gadad BS, Britton GB, Rao KS. Targeting oligomers in neurodegenerative disorders: lessons from alpha-synuclein, tau, and amyloid-beta peptide. *J Alzheimers Dis* 2011;24(Suppl 2):223–232.
42. Wagner J, Ryazanov S, Leonov A, et al. Anle138b: a novel oligomer modulator for disease-modifying therapy of neurodegenerative diseases such as prion and Parkinson's disease. *Acta Neuropathol* 2013;125:795–813.
43. Wagner J, Krauss S, Shi S, et al. Reducing tau aggregates with anle138b delays disease progression in a mouse model of tauopathies. *Acta Neuropathol* 2015;130:619–631.
44. Levin J, Schmidt F, Boehm C, et al. The oligomer modulator anle138b inhibits disease progression in a Parkinson mouse model even with treatment started after disease onset. *Acta Neuropathol* 2014;127:779–780.
45. Martinez Hernandez A, Urbanke H, Gillman AL, et al. The diphenylpyrazole compound anle138b blocks Abeta channels and rescues disease phenotypes in a mouse model for amyloid pathology. *EMBO Mol Med* 2018;10:32–47.
46. Fleming SM, Salcedo J, Fernagut PO, et al. Early and progressive sensorimotor anomalies in mice overexpressing wild-type human alpha-synuclein. *J Neurosci* 2004;24:9434–9440.
47. Fleming SM, Ekhatior OR, Ghisays V. Assessment of sensorimotor function in mouse models of Parkinson's disease. *J Vis Exp* 2013;(76):50303.
48. Stefanova N, Kaufmann WA, Humpel C, Poewe W, Wenning GK. Systemic proteasome inhibition triggers neurodegeneration in a transgenic mouse model expressing human alpha-synuclein under oligodendrocyte promoter: implications for multiple system atrophy. *Acta Neuropathol* 2012;124:51–65.
49. Zotova E, Bharambe V, Cheaveau M, et al. Inflammatory components in human Alzheimer's disease and after active amyloid-beta42 immunization. *Brain* 2013;136(Pt 9):2677–2696.
50. Doorn KJ, Moors T, Drukarch B, van de Berg W, Lucassen PJ, van Dam AM. Microglial phenotypes and toll-like receptor 2 in the substantia nigra and hippocampus of incidental Lewy body disease cases and Parkinson's disease patients. *Acta Neuropathol Commun* 2014;2:90.
51. Theodore S, Cao S, McLean PJ, Standaert DG. Targeted overexpression of human alpha-synuclein triggers microglial activation and an adaptive immune response in a mouse model of Parkinson disease. *J Neuropathol Exp Neurol* 2008;67:1149–1158.
52. Fellner L, Irschick R, Schanda K, et al. Toll-like receptor 4 is required for alpha-synuclein dependent activation of microglia and astroglia. *Glia* 2013;61:349–360.
53. Guerrero-Munoz MJ, Castillo-Carranza DL, Kaye R. Therapeutic approaches against common structural features of toxic oligomers shared by multiple amyloidogenic proteins. *Biochem Pharmacol* 2014;88:468–478.
54. Valera E, Spencer B, Masliah E. Immunotherapeutic approaches targeting amyloid-beta, alpha-synuclein, and tau for the treatment of neurodegenerative disorders. *Neurotherapeutics* 2016;13:179–189.
55. Lashuel HA, Hartley D, Petre BM, Walz T, Lansbury PT, Jr. Neurodegenerative disease: amyloid pores from pathogenic mutations. *Nature*. 2002;418:291.
56. Lotharius J, Brundin P. Pathogenesis of Parkinson's disease: dopamine, vesicles and alpha-synuclein. *Nat Rev Neurosci* 2002;3:932–942.
57. Kim C, Ho DH, Suk JE, et al. Neuron-released oligomeric alpha-synuclein is an endogenous agonist of TLR2 for paracrine activation of microglia. *Nat Commun* 2013;4:1562.
58. Lee HJ, Bae EJ, Lee SJ. Extracellular alpha-synuclein—a novel and crucial factor in Lewy body diseases. *Nat Rev Neurol* 2014;10:92–98.
59. Zhang W, Wang T, Pei Z, et al. Aggregated alpha-synuclein activates microglia: a process leading to disease progression in Parkinson's disease. *FASEB J* 2005;19:533–542.
60. Fellner L, Kuzdas-Wood D, Levin J, et al. Anle138b partly ameliorates motor deficits despite failure of neuroprotection in a model of advanced multiple system atrophy. *Front Neurosci* 2016;10:99.

## Supporting Data

Additional Supporting Information may be found in the online version of this article at the publisher's web-site.